analytical chemistry

Article

Cite This: *Anal. Chem.* 2019, 91, 13458−13464

pubs.acs.org/ac

Selective Determination of Isothermally Amplified Zika Virus RNA Using a Universal DNA-Hairpin Probe in Less than 1 Hour

Charles A. Lynch III,[†,‡,§] Marcos V. Foguel,[†,§] Adam J. Reed,[†] Angelica M. Balcarcel,[†] Percy Calvo-Marzal,[†] Yulia V. Gerasimova,[†] and Karin Y. Chumbimuni-Torres*[,†]

[†]Department of Chemistry, University of Central Florida, 4000 Central Florida Boulevard, Orlando, Florida 32816, United States

[‡]Rose Hulman Institute of Technology, 5500 Wabash Avenue, Terre Haute, Indiana 47803, United States

Supporting Information

ABSTRACT: The recent outbreak of the Zika virus (ZIKV) in the Americas and multiple studies that linked the virus to the cases of microcephaly and neurological complications have revealed the need for cost efficient and rapid ZIKV diagnostics tests. Here, a diagnostic platform relying on a four-way junction (4WJ)-based biosensor with electrochemical readout using a Universal DNA-Hairpin (UDH) probe for the selective recognition of an isothermally amplified ZIKV RNA fragment is developed. The 4WJ structure utilizes an electrode-immobilized stem-loop (DNA-hairpin) probe and two DNA adaptor strands complementary to both the stem-loop probe and the targeted fragment of a ZIKV amplicon. One of the adaptor strands is responsible for high selectivity of the target recognition, while another helps unwinding the target secondary structure. The first adaptor strand contains a redox label methylene blue to trigger the current change in response to the target-dependent formation of the 4WJ structure on the surface of the electrode. The amplicon can be analyzed directly from the amplification sample without the need for its purification. The proposed diagnostic methodology exhibits the limit of ZIKV RNA detection of 1.11 fg/μL (∼0.3 fM) and high selectivity that allows for reliable discrimination of ZIKV from West Nile virus and four dengue virus serotypes. Overall, the analysis of ZIKV RNA can be completed in less than 1 h, including amplification and electrochemical detection.

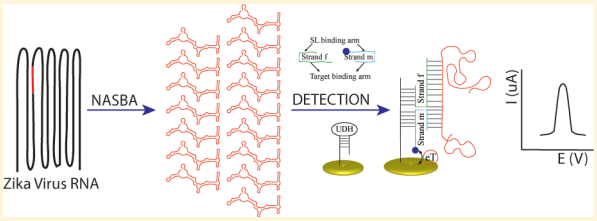

Recently, there have been outbreaks of the Zika virus (ZIKV) infection in the Americas and Caribbean. The new cases of ZIKV infections were characterized by higher virulence and more severe complications than previously observed.[1−3] It has been confirmed that the causative agents of these infections are related to the Asian lineage of the virus that have evolved in the Americas.[4−6] ZIKV from the Asian lineage has been shown to be less virulent than the isolates belonging to the African lineage; however, it is associated with neuronal malfunctions.[5] Acute ZIKV infection as a risk factor for the neurological disease Guillain−Barré syndrome has been reported in Puerto Rico,[7] as well as other affected countries.[2] There is also a correlation between ZIKV and incidents of microcephaly in newborns of women infected with the virus, which have been reported in Brazil, Colombia, and the United States.[3,8,9] According to the Center for Disease Control (CDC), over 4 900 pregnant women with the laboratory evidence of possible ZIKV infection have been reported in the U.S. territories and freely associated states since 2015.[10] Of those pregnancies, 175 have resulted in pregnancy losses or liveborn infants with ZIKV-associated birth defects.[11] Even though there is currently no specific treatment to decrease the chances of the complication development, and the current adult morbidity rate is low, timely diagnosis of the ZIKV infections in the Americas can prevent spreading of the virus and assist in the virus monitoring and surveillance.

Several recent reports have highlighted the advancement in technology for ZIKV detection, as well as concerns for monitoring the spread of the virus in the future.[12−14] Currently recommended approaches for the ZIKV detection include enzyme-linked immunosorbent assays (ELISA)[15,16] and nucleic acid amplification tests (NAATs).[17,18] A serious disadvantage of ELISA-based methods is cross-reactivity between ZIKV and other flavivirus, such as dengue virus (DENV) and West Nile virus (WNV), which limits the use of immunoassays for ZIKV diagnostics.[19−22] Additionally, these methods are able to detect the infection only after the acute phase. NAATs, on the contrary, selectively detect the virus's presence in biological fluids shortly after infection. Currently used NAATs mostly rely on the reverse transcription-polymerase chain reaction (RT-PCR),[23,24] which is time-consuming and requires sophisticated equipment and highly trained personnel, thus making it difficult to transition the diagnostics from the laboratory to point-of-care tests (POCT).

Electrochemical detection of virus-specific nucleic acid sequences offers advantages of cost-efficiency, ease of implementation, detector portability, high selectivity and ability to detect a targeted nucleic acid in the fM range.[25−27] Recently, we have reported on an electrochemical biosensor

Received: May 27, 2019
Accepted: October 1, 2019
Published: October 1, 2019

DOI: 10.1021/acs.analchem.9b02455
Anal. Chem. 2019, 91, 13458−13464

utilizing a four-way junction (4WJ) platform for the detection of miRNA, ssDNA of 60−200 nt with capability of discriminating single-nucleotide substitutions, and a single electrochemical biosensor for different DNA analytes.[28−30] We have demonstrated such advantages of the 4WJ-based biosensor as its ability to detect nucleic acid sequences with secondary structures, the unique design that explores a universal DNA-hairpin probe allowing the possibility to reuse the biosensor. The aim of this study is to develop a diagnostic platform based on an isothermal amplification of a fragment of ZIKV RNA and direct analysis of the amplicon using the ZIKV-specific 4WJ-based electrochemical biosensor. Here, we optimized both the amplification and detection step of the platform, determined the limit of detection and sensitivity, and proved the high selectivity of the diagnostic platform by reliably differentiating ZIKV RNA from that of other flaviviruses (DENV, WNV). The developed platform is promising for diagnostics of ZIKV infection, potentially as a POCT.

EXPERIMENTAL SECTION

Materials. Oligonucleotides used as primers, biosensor strands and probe, or synthetic target mimics were purchased from Integrated DNA Technologies (Coralville, IA). The m adaptor strand modified with a methylene blue (MeB) redox marker was purchased from Biosearch Technologies, Inc. (Petaluma, CA). All oligonucleotides used are shown in Table S1 (Supporting Information). Trizma hydrochloride (Tris-HCl), tris(2-carboxyethyl) phosphine hydrochloride (TCEP), 6-mercapto-1-hexanol (MCH), and $MgCl_2$ were purchased from Sigma-Aldrich (St. Louis, MO). Sodium chloride, sodium hydroxide, and sulfuric acid were obtained from Fisher Scientific (Pittsburgh, PA). Gold disc electrodes (GDEs) were purchased from CH Instruments (Austin, TX). Alumina slurry (1.0 μm, 0.3 μm, and 0.05 μm) was obtained from Buehler (Lake Bluff, IL). All aqueous solutions were prepared with deionized water (18 MΩ cm) using a Siemens PURELAB Ultra system (Lowell, MA). The immobilization buffer (IB) was prepared with 50 mM Tris-HCl and 250 mM NaCl and adjusted to a pH of 7.4 using 1.0 M NaOH. The hybridization buffer (HB) was prepared with 50 mM Tris-HCl, 100 mM NaCl, and 50 mM $MgCl_2$ and adjusted to pH 7.4 using 1.0 M NaOH.

NASBA Reaction. Viral RNA isolated from Vero cells infected with ZIKV (strain PRVABC-59, Genbank accession no. KX377337) was used as a template for nucleic acid sequence-based amplification (NASBA) at 5, 50, or 500 fg/μL (~1.34, 13.4, and 134 fM) concentrations. The reaction was performed using a NASBA kit (Life Sciences Advanced Technologies, Inc., St. Petersburg, FL) and 250 nM primers (Table S1). The total volume of each reaction mixture was 15 μL. The reaction conditions were as recommended by the vendor with time variations from 15 to 45 min. For virus discrimination experiments, RNA (50 fg/μL) isolated from WNV (strain NY99) or DENV serotypes 1−4 (strains Hawaii, New Guinea C, BR327, H241, respectively) was used as a template for NASBA reaction with ZIKV primers. Samples were analyzed by electrophoresis in 2% agarose gel containing Gel Red (Biotium, Fremont, CA) for band visualization (Figure S1). The gel images were analyzed using a BioRad Gel Doc XR+ with Image Lab software. To build the calibration curve of a ZIKV RNA fragment, ZIKV NASBA amplicon was used as a target, which was isolated and purified from other components of the amplification reaction mixture with E.Z.N.A. MicroElute RNA clean up kit (Omega Biotek, Inc., Norcross, GA). The concentration of the isolated RNA amplicon (also called standard amplicon) was determined by measuring the absorbance of the amplicon solution at 260 nm and considering that ~40 μg/mL RNA solution would have an absorbance of 1.0.

Electrochemical Measurements. Square wave voltammetry (SWV) was performed with a CHI660D Electrochemical Workstation. A typical three-electrode system was used, where the modified GDE, a platinum wire and Ag/AgCl (1 M KCl) were used as working, counter, and reference electrodes, respectively. SWV measurements were recorded in HB at a potential range from 0.0 to −0.5 V, frequency of 100 Hz, amplitude of 70 mV, and step potential of 3 mV. Nitrogen was bubbled into the electrochemical cell to remove oxygen before the measurements were conducted. All the measurements were performed in triplicate at room temperature.

Biosensor Preparation. GDEs were used as the substrate for a Universal DNA-Hairpin (UDH) probe immobilization. Before every analysis, the electrodes were cleaned by their immersion in piranha solution (1:3 ratio of 30% H_2O_2−98% H_2SO_4) for 10 min. Subsequently, the electrodes were manually polished on a microcloth with an alumina slurry (1.0, 0.3, and 0.05 μm), rinsed with water, and sonicated in water and ethanol to remove any residual alumina particles trapped on the electrode surface. Finally, the GDE were activated in 0.5 M H_2SO_4 via cyclic voltammetry from 1.6 to −0.1 V at a scan rate of 100 mV/s. This last step was used to accurately calculate the electrochemically active area of each electrode.

Disulfide bond of the UDH was reduced with 1.0 mM TCEP by shaking the solution at room temperature for 1 h. Then, the solution was further diluted to 0.1 μM of the UDH in IB solution, and 15 μL of this solution was drop-casted on to the GDEs for 30 min. Afterward, the electrode surface was rinsed and dried with nitrogen, and 15 μL of 2 mM MCH in IB was drop-casted and incubated for 30 min. Hybridization of the UDH probe with other biosensor components was performed using 0.5 μM f-strand, 0.25 μM m-strand, and different concentrations of the target, which was either synthetic ZIKV ssDNA strand (138 nt) or ZIKV RNA amplicon (~147 nt), in HB. For the analysis, 15 μL of the mixture solution (m- and f-strands + target) was drop-casted onto the electrode. The biosensor response was expressed as the current density peak (j_p) calculated as the current signal for a sample minus the current for the baseline.

Biosensor Characterization. For initial characterization and optimization of the electrochemical biosensor, a synthetic DNA target mimicking a product of NASBA reaction upon ZIKV RNA amplification was used. To accomplish this, the UDH probe immobilized on the electrode surface was incubated with f-strand (0.5 μM), m-strand (0.25 μM), and either in the absence or presence of DNA target (50 nM) in HB at room temperature. Hybridization time was evaluated at 1, 2.5, 5, 10, 20, 30, 60, and 90 min. Control experiments lacking one or more components were also performed. The control samples were prepared in the absence of (1) UDH, (2) f-strand, (3) target, or (4) both f-strand and target. Calibration curves for synthetic ZIKV DNA and purified ZIKV RNA amplicon were obtained from 1 to 75 nM. Lastly, the selectivity of the biosensor was evaluated using 50 nM synthetic DENV ssDNA (114 nt) as a target instead of ZIKV DNA.

DOI: 10.1021/acs.analchem.9b02455
Anal. Chem. 2019, 91, 13458−13464

Detection of NASBA Products. Reaction mixtures from the NASBA reactions using either ZIKV, DENV, or WNV RNA as a template and ZIKV-specific primers were added at 10% (v/v) to a 50 μL sample containing 0.5 μM f-strand and 0.25 μM m-strand in HB. Then, an aliquot of 15 μL of the sample was applied to each GDE previously modified with the UDH probe. The biosensor was then incubated for 10 min at room temperature followed by measuring the electrochemical signal as described above. The signal from three replicates was averaged.

RESULTS AND DISCUSSION

A biosensor based on the 4WJ platform is designed as shown in Figure 1. The biosensor contains a universal DNA-hairpin

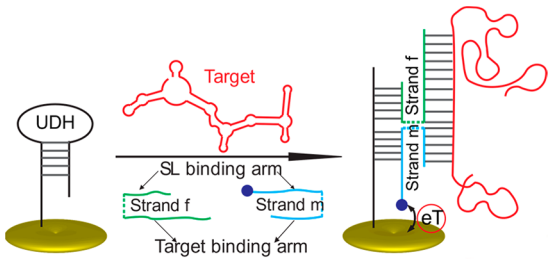

Figure 1. Scheme of the 4WJ-based biosensor.

Probe UDH immobilized on the surface of a GDE via a thiol bond, followed by backfilling with a monolayer of a short chain organic compound (MCH) to avoid nonspecific adsorption. In addition, two adaptor strands (m and f) are used, each of which contains one fragment complementary to the UDH probe and another fragment complementary to a fragment of the ZIKV genome (target). These adaptor strands hybridize to the UDH only in the presence of target. One of the adaptor strands (m-strand) is modified with a redox marker methylene blue (MeB). Formation of the 4WJ structure in the presence of the viral target brings the redox marker close to the GDE surface to enable electron transfer (eT), thereby allowing for an electrochemical signal to be measured. An important feature of the m-strand is that its target-binding fragment is relatively short and thus binds only to the fully complementary target fragment under the analysis conditions (in the presence of f-strand). This fragment (m-strand) ensures high selectivity of the biosensor and its capability to differentiate between even closely related target sequences down to single nucleotide variations.[31−35] The other adaptor strand, f-strand, has a longer target-binding fragment to efficiently unwind the target's secondary structure.[33,36−38] The 4WJ structure formation was previously characterized using spectroscopic ellipsometry.[28]

Biosensor Response. The biosensor performance was first evaluated using a 138-nt synthetic DNA target (ZIKV T-138) mimicking a fragment of the ZIKV RNA and containing the sequence of nt 2681−2711 of the viral genome (strain PRVABC-59), which is recognized by the biosensor adaptor strands. The time needed for the target and adaptor strands to hybridize with the UDH probe immobilized on the GDE was optimized. It was observed that while the signal could be measured almost immediately (within 1 min) after depositing the mixture of the target with the adaptor strands to the electrode, prolonged hybridization time resulted in a considerable increase of the target-dependent response (Figure S2). To minimize the time the detection stage, 10 min of hybridization time was chosen for the subsequent experiments, since more than a 10-fold increase of the signal over the blank (no target present) was achieved under these conditions, which is enough for reliable target detection.[39]

Control experiments were performed to verify the response of the biosensor in the absence of the target and/or other components of the 4WJ ensemble. Indeed, the biosensor exhibited a significant electrochemical response only in the presence of all components required to form the 4WJ structure, while the absence of any component resulted in a negligible signal (Figure S3). Additionally, gel electrophoresis experiments showed formation of a low-mobility complex at approximately 150 bp, which can be assigned to as the 4WJ structure only when all components of the 4WJ were present (Figure S4). The electrochemical response of the biosensor depended linearly on the target concentration in the range of 1−75 nM ZIKV T-138 (Figure S5) with a sensitivity of 0.068 μA/cm^2 nM (the slope of the linear trendline) and a limit of detection (LOD) of 1.24 nM (calculated as 3 times the standard deviation of the blank divided by the slope from the calibration curve). No signal was observed when target DENV T-114, which mimicked an amplicon of DENV genome corresponding to the biosensor-targeting fragment, was analyzed (Figure S6).

To build the calibration curve of the ZIKV RNA fragment, ZIKV NASBA standard amplicon was used as a target, which was previously isolated and purified. Based on the obtained calibration curve (Figure 2), a linear range from 1 to 75 nM

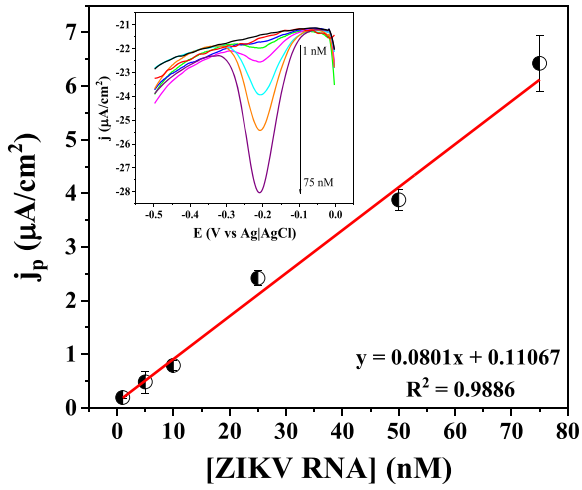

Figure 2. Biosensor calibration curve for ZIKV RNA target after immobilization of the UDH probe, backfilling with MCH, and hybridization with adaptor strands (m and f) for varied concentrations (1, 5, 10, 25, 50, and 75 nM) of RNA amplicon with 10 min of hybridization time. Inset: Corresponding SWV for each of the concentration in the calibration curve, and the background (UDH + MCH, black line) and the blank response (UDH + strands m and f, red line).

was obtained with a sensitivity of 0.080 μA/cm^2 nM and a LOD of 0.99 nM. This LOD corresponds to the lowest concentration of the RNA amplicon that can be distinguished by the biosensor from the absence of the amplicon (blank) with a 99% confidence level.[40]

Amplification of a ZIKV Genome Fragment. It has been reported that ZIKV RNA can be found in biofluids up to picomolar concentrations,[41,42] so a step for amplification of

DOI: 10.1021/acs.analchem.9b02455
Anal. Chem. 2019, 91, 13458−13464

viral RNA is required prior to the target detection using the electrochemical 4WJ-based biosensor. For the biosensor to be used for POCT, an isothermal method that does not require a long time and sophisticated equipment for the viral RNA amplification should be used. NASBA reaction, which has been previously suggested for amplification of RNA fragments,[43−45] is very promising in the case of RNA viruses, such as ZIKV. This isothermal amplification techniques relies on the activities of three enzymes, reverse transcriptase, RNase H, and T7 RNA polymerase, to efficiently copy a desired fragment of the viral genome.[46] As a result, a single-strand RNA amplicon at micromolar concentrations is obtained and can be conveniently interrogated by the designed 4WJ-based electrochemical biosensor.

To amplify a fragment of ZIKV genomic RNA, we used previously designed primers targeting the envelope gene of the virus.[44] A standard protocol for the NASBA reaction requires incubation of the viral RNA with a set of primers, one of which contains a T7 promotor, a mixture of NTPs and dNTPs, and the enzymes at 41 °C for up to 3 h.[46] In order to reduce the total analysis time including RNA amplification and the amplicon detection, we optimized the amplification time. Thus, NASBA reaction was performed for 15, 30, or 45 min followed by the amplicon detection with the 4WJ-based biosensor (Figure 3). Longer amplification, for more than 45 min, resulted in higher electrochemical signal (data not shown). However, to shorten the total analysis time and reliably distinguish the signal in the target's presence from the blank, 45 min was chosen for further experiments. Thus, the total analysis time to detect ZIKV RNA allotting for amplification, hybridization, and detection with the biosensor is shorten to 1 h (45 min of amplification + 10 min of hybridization to form the 4WJ structure + 1 min of detection). Notice that in Figure 3, the current density peak obtain with the 4WJ-based biosensor displays a 25-fold increase (4.9 ± 0.3 $\mu A/cm^2$) in the presence of the target amplicon after 45 min of NASBA when compared to the negative control (0.19 ± 0.09 $\mu A/cm^2$), when no RNA was added to NASBA reaction. Resulting in an amplification efficiency of 10^6 from ZIKV RNA concentration of 50 fg/μL (~13.4 fM) to an amplicon target concentration on the order of nanomolar, since 4.9 $\mu A/cm^2$ correspond to 60 nM in the calibration curve of Figure 2.

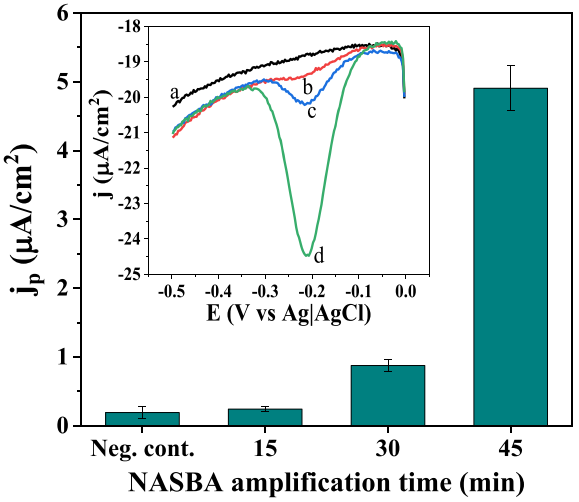

Figure 3. Biosensor response to the NASBA negative control (no viral RNA added to the amplification mixture) or NASBA samples with ZIKV RNA (50 fg/μL) amplified for 15, 30, and 45 min. Both the negative control and samples were used at 10% (v/v). Inset: SWV response of a GDE/UDH with MCH backfill layer (a) or after hybridization of the 4WJ-based biosensor with ZIKV NASBA amplicon amplified for 15 (b), 30 (c), or 45 min (d).

Selectivity. Due to high homology between the genomes of ZIKV and other flaviviruses, it is important to ensure no cross-reaction is observed in the presence of nonspecific viral RNA. Therefore, the selectivity of the proposed methodology was evaluated using both synthetic target mimics (Figure S6) and NASBA amplicons (Figure 4). NASBA of Puerto Rican ZIKV isolate (ZIKV-PR), Brazilian ZIKV isolate (ZIKV-BR), DENV (serotypes 1−4), or WNV was done with ZIKV primers. NASBA was also performed and evaluated using mixtures of ZIKV-PR with DENV1 or ZIKV-PR with WNV.

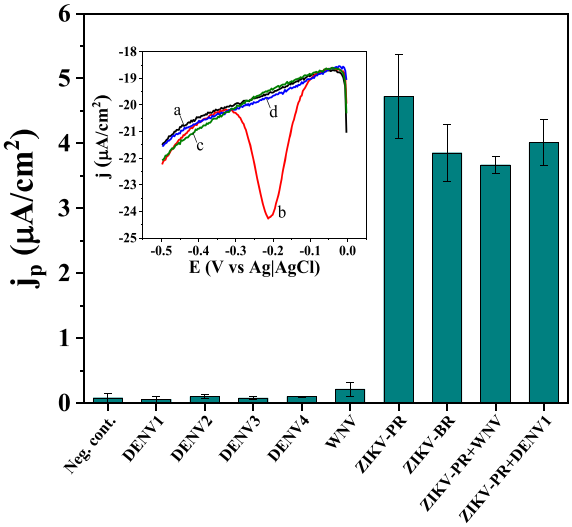

Figure 4. Biosensor response to NASBA negative control (Neg. cont.); NASBA products from either WNV, DENV1, DENV2, DENV3, or DENV4 RNA amplification; NASBA ZIKV amplicons from Puerto Rican (ZIKV-PR) or Brazilian (ZIKV-BR) isolates; and NASBA product from ZIKV-PR + WNV or ZIKV + DENV1 mixtures. NASBA reaction was performed for 45 min using 50 fg/μL RNA; all samples were used at 10% (v/v) final concentration for the electrochemical analysis. Inset: SWV response of a GDE/UDH with MCH backfill layer after incubation of the adaptor strands and NASBA Negative Control (a), NASBA ZIKV-PR amplicon (b), or the NASBA products of DENV2 (c) or WNV (d) RNA using ZIKV-specific primers.

As shown in Figure 4, the samples that contain ZIKV (ZIKV-PR or ZIKV-BR) and mixtures (ZIKV plus DENV1 and ZIKV plus WNV) were the only ones that triggered a significant electrochemical signal, with the current density peak higher than 3.5 $\mu A/cm^2$. Other analyzed samples exhibited negligible response, with the current density peak of 0.12 ± 0.05 $\mu A/cm^2$ and 0.2 ± 0.1 $\mu A/cm^2$ for NASBA negative control and WNV NASBA product, respectively. For the samples containing NASBA amplicons from either DENV serotype, the signal was lower or close to the current density peak obtained for the negative control. Therefore, the biosensor demonstrated the ability to differentiate isolates of ZIKV RNA from other flaviviruses, even in the presence of nonspecific RNA.

Signal Dependence on Viral RNA Concentration. To verify that the developed methodology is suitable for the

DOI: 10.1021/acs.analchem.9b02455
Anal. Chem. 2019, 91, 13458−13464

detection of clinically relevant concentrations of ZIKV RNA, we varied the RNA concentration (5, 50, or 500 fg/μL) used for a 45 min NASBA reaction. The amplicon samples (10% v/v) were then analyzed using the 4WJ-based biosensor (Figure 5).

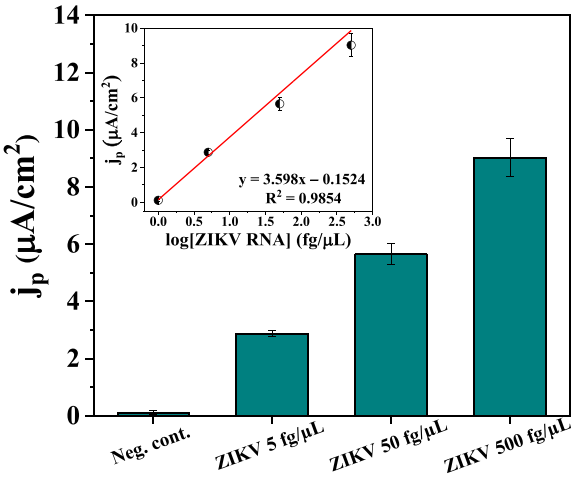

Figure 5. Biosensor response to the NASBA negative control or NASBA samples obtained using 5, 50, and 500 fg/μL ZIKV RNA; all samples were amplified for 45 min and added to the biosensor at 10% (v/v) final concentration. Inset: Dependence of the biosensor response on the logarithm of ZIKV RNA concentration taken for the amplification step. The data for three independent NASBA samples were used to obtain the calibration curve.

For a sample amplified from 5 fg/μL (~1.34 fM) ZIKV RNA, the current density peak of 2.9 ± 0.1 μA/cm^2 was observed, which represents more than 20-fold increase over the negative control signal. The samples obtained using 50 fg/μL (~13.4 fM) and 500 fg/μL (~134 fM) ZIKV RNA exhibited a signal of j_p = 5.7 ± 0.4 μA/cm^2 and 9.0 ± 0.7 μA/cm^2, respectively. The signal was shown to depend linearly on the logarithm of the initial (preamplified) RNA concentration (Figure 5, inset), due to the presumed exponential amplification of the viral RNA using the NASBA reaction. From the calibration curve obtained with three independent NASBA samples (performed at different days), the LOD for the entire method (RNA amplification + electrochemical detection) was 1.11 fg/μL (~0.3 fM). This value is the lowest possible concentration of viral RNA to be taken for amplification and subsequent analysis of the amplicon by the 4WJ electrochemical biosensor. Based on the estimated molar mass of the ZIKV genome (~3.7 × 10^6 g/mol), the LOD corresponds to 1.8 × 10^5 ZIKV RNA copies/mL). The calculated LOD for the entire method is lower than the concentration found in clinical samples, as reported in the literature[41,42] (about 7 × 10^5 copies/mL), showing the potentiality of the method for detection of ZIKV in real samples. Further experiments are underway in our laboratory in this regard. The repeatability of the method was successful, since the coefficient of variation (% CV) calculated was between 3.7 and 7.4%. Therefore, the developed system for ZIKV detection can not only selectively detect the presence of ZIKV RNA but also estimate viral RNA concentration in the samples.

There are few publications reporting electrochemical biosensors for nucleic acid-based ZIKV detection. A comparison of the proposed biosensor with these works is shown in Table 1. The LOD for all reported biosensors was higher than that for the biosensor proposed in this work, which demonstrates the importance of coupling the electrochemical detection to a nucleic acid amplification technique to obtain a lower LOD. It is also noteworthy that the addition of NASBA did not make the analysis process longer, as the assay time of the proposed methodology was similar to those reported in other works.

CONCLUSION

A four-way junction electrochemical biosensor was designed and optimized to selectively detect Zika virus circulated in the Americas. The biosensor successfully interrogated the product of isothermal ZIKV RNA amplification directly in the amplification samples with good repeatability and the LOD of 1.11 fg/μL (~0.3 fM or 1.8 × 10^5 ZIKV RNA copies/mL) viral RNA and the ability to discriminate between RNA sequences of ZIKV, WNV and DENV types 1−4 using the same NASBA protocol. The developed system has a potential for estimation of viral RNA concentration in the samples. The complete analysis, including both RNA amplification and electrochemical detection of the targeted ZIKV RNA fragment, can be completed within 1 h, which is comparable with a regular visit to doctor's office. Thus, our findings demonstrate the potential of the 4WJ-based electrochemical biosensor for point-of-care clinical diagnostics of ZIKV infection.

ASSOCIATED CONTENT

Supporting Information

The Supporting Information is available free of charge on the ACS Publications website at DOI: 10.1021/acs.analchem.9b02455.

Table 1. Comparison of the Electrochemical Biosensors Based on DNA/RNA for ZIKV Detection Reported in the Literature

technique	platform	LOD	assay time (min)	ref
nucleic acid sequence-based amplification (NASBA)/ square wave voltammetry	UDH immobilized on gold electrodes to form 4WJ structure	0.3 fM	55	this work
electrochemical impedance spectroscopy	thiol-probe DNA immobilized on ox-GCE-[AuNPs-SiPy][a] for target hybridization	820 fM	50	47
square wave voltammetry	poly(3-amino-4-hydroxybenzoic acid)-modified pencil carbon graphite electrode activated with EDC/NHS[b] for probe immobilization	2.54 × 10^4 fM	45	48
electrochemical impedance spectroscopy	thiol-probe DNA immobilized on gold-PET electrodes for target hybridization	2.5 × 10^7 fM	90	49

[a]Oxidized glassy carbon electrode modified with silsesquioxane-functionalized gold nanoparticles. [b]1-Ethyl-3-(3-(dimethylamino)propyl) carbodiimide hydrochloride (EDC)/ *N*-hydroxysuccinimide (NHS).

DOI: 10.1021/acs.analchem.9b02455
Anal. Chem. 2019, 91, 13458−13464

Oligonucleotides sequences, agarose gel electrophoretic analysis of NASBA products, optimization of hybridization time, and data of the control experiment on biosensor component requirement (PDF)

AUTHOR INFORMATION

Corresponding Author

*E-mail: Karin.ChumbimuniTorres@ucf.edu.

ORCID

Yulia V. Gerasimova: 0000-0001-8804-9770

Karin Y. Chumbimuni-Torres: 0000-0001-5564-3829

Author Contributions

§C.A.L. III and M.V.F. contributed equally.

Notes

The authors declare no competing financial interest.

ACKNOWLEDGMENTS

The authors acknowledge NSF-CBET Grant Number 1706802 and Florida Health Department Grant Numbers 7ZK05 and 7ZK33. The authors are thankful to Dr. Hyeryun Choe (Scripps Research Institute, Jupiter, FL) for providing viral RNA.

REFERENCES

(1) Musso, D.; Gubler, D. J. *Clin. Microbiol. Rev.* **2016**, *29* (3), 487−524.

(2) Galán-Huerta, K. A.; Rivas-Estilla, A. M.; Martinez-Landeros, E. A.; Arellanos-Soto, D.; Ramos-Jiménez, J. *Medicina Universitaria* **2016**, *18* (71), 115−124.

(3) Faria, N. R.; Azevedo, R. d. S. d. S.; Kraemer, M. U. G.; Souza, R.; Cunha, M. S.; Hill, S. C.; Theze, J.; Bonsall, M. B.; Bowden, T. A.; Rissanen, I.; Rocco, I. M.; Nogueira, J. S.; Maeda, A. Y.; Vasami, F. G. d. S.; Macedo, F. L. d. L.; Suzuki, A.; Rodrigues, S. G.; Cruz, A. C. R.; Nunes, B. T.; Medeiros, D. B. d. A.; Rodrigues, D. S. G.; Nunes Queiroz, A. L.; Silva, E. V. P. d.; Henriques, D. F.; Travassos da Rosa, E. S.; de Oliveira, C. S.; Martins, L. C.; Vasconcelos, H. B.; Casseb, L. M. N.; Simith, D. d. B.; Messina, J. P.; Abade, L.; Lourenco, J.; Alcantara, L. C. J.; Lima, M. M. d.; Giovanetti, M.; Hay, S. I.; de Oliveira, R. S.; Lemos, P. d. S.; Oliveira, L. F. d.; de Lima, C. P. S.; da Silva, S. P.; Vasconcelos, J. M. d.; Franco, L.; Cardoso, J. F.; Vianez-Junior, J. L. d. S. G.; Mir, D.; Bello, G.; Delatorre, E.; Khan, K.; Creatore, M.; Coelho, G. E.; de Oliveira, W. K.; Tesh, R.; Pybus, O. G.; Nunes, M. R. T.; Vasconcelos, P. F. C. *Science* **2016**, *352* (6283), 345−349.

(4) Logan, I. S. *Zool. Res.* **2016**, *37* (2), 110−115.

(5) Tripathi, S.; Balasubramaniam, V. R.; Brown, J. A.; Mena, I.; Grant, A.; Bardina, S. V.; Maringer, K.; Schwarz, M. C.; Maestre, A. M.; Sourisseau, M.; Albrecht, R. A.; Krammer, F.; Evans, M. J.; Fernandez-Sesma, A.; Lim, J. K.; Garcia-Sastre, A. *PLoS Pathog.* **2017**, *13* (3), No. e1006258.

(6) Ye, Q.; Liu, Z. Y.; Han, J. F.; Jiang, T.; Li, X. F.; Qin, C. F. *Infect., Genet. Evol.* **2016**, *43*, 43−9.

(7) Dirlikov, E.; Major, C. G.; Medina, N. A.; Lugo-Robles, R.; Matos, D.; Munoz-Jordan, J. L.; Colon-Sanchez, C.; Garcia, M.; Olivero-Segarra, M.; Malave, G.; Rodriguez-Vega, G. M.; Thomas, D. L.; Waterman, S. H.; Sejvar, J. J.; Luciano, C. A.; Sharp, T. M.; Rivera-Garcia, B. *JAMA Neurol* **2018**, *75* (9), 1089−1097.

(8) Walker, C. L.; Little, M. E.; Roby, J. A.; Armistead, B.; Gale, M., Jr.; Rajagopal, L.; Nelson, B. R.; Ehinger, N.; Mason, B.; Nayeri, U.; Curry, C. L.; Adams Waldorf, K. M. *Am. J. Obstet. Gynecol.* **2019**, *220* (1), 45−56.

(9) Alvarado-Socarras, J. L.; Idrovo, A. J.; Contreras-Garcia, G. A.; Rodriguez-Morales, A. J.; Audcent, T. A.; Mogollon-Mendoza, A. C.; Paniz-Mondolfi, A. *Travel Med. Infect Dis* **2018**, *23*, 14−20.

(10) *CDC Pregnant Women with Any Laboratory Evidence of Possible Zika Virus Infection, 2015−2018*, https://www.cdc.gov/pregnancy/zika/data/pregwomen-uscases.html.

(11) *CDC Outcomes of Pregnancies with Laboratory Evidence of Possible Zika Virus Infection, 2015−2018*, https://www.cdc.gov/pregnancy/zika/data/pregnancy-outcomes.html.

(12) Peters, R.; Stevenson, M. *Clin. Microbiol. Infect.* **2019**, *25* (2), 142−146.

(13) Grubaugh, N. D.; Ladner, J. T.; Lemey, P.; Pybus, O. G.; Rambaut, A.; Holmes, E. C.; Andersen, K. G. *Nat. Microbiol* **2019**, *4* (1), 10−19.

(14) Chotiwan, N.; Brewster, C. D.; Magalhaes, T.; Weger-Lucarelli, J.; Duggal, N. K.; Ruckert, C.; Nguyen, C.; Garcia Luna, S. M.; Fauver, J. R.; Andre, B.; Gray, M.; Black, W. C. t.; Kading, R. C.; Ebel, G. D.; Kuan, G.; Balmaseda, A.; Jaenisch, T.; Marques, E. T. A.; Brault, A. C.; Harris, E.; Foy, B. D.; Quackenbush, S. L.; Perera, R.; Rovnak, J. *Sci. Transl. Med.* **2017**, *9* (388), eaag0538.

(15) Granger, D.; Hilgart, H.; Misner, L.; Christensen, J.; Bistodeau, S.; Palm, J.; Strain, A. K.; Konstantinovski, M.; Liu, D.; Tran, A.; Theel, E. S. *J. Clin. Microbiol.* **2017**, *55* (7), 2127−2136.

(16) Muller, J. A.; Harms, M.; Schubert, A.; Mayer, B.; Jansen, S.; Herbeuval, J. P.; Michel, D.; Mertens, T.; Vapalahti, O.; Schmidt-Chanasit, J.; Munch, J. *Med. Microbiol. Immunol.* **2017**, *206* (2), 175−185.

(17) *CDC Revised diagnostic testing for Zika, chikungunya, and dengue viruses in US Public Health Laboratories*, https://stacks.cdc.gov/view/cdc/38149.

(18) Powell, L.; Wiederkehr, R. S.; Damascus, P.; Fauvart, M.; Buja, F.; Stakenborg, T.; Ray, S. C.; Fiorini, P.; Osburn, W. O. *Analyst* **2018**, *143* (11), 2596−2603.

(19) Basile, K.; Kok, J.; Dwyer, D. E. *Pathology* **2017**, *49* (7), 698−706.

(20) Charrel, R. N.; Leparc-Goffart, I.; Pas, S.; de Lamballerie, X.; Koopmans, M.; Reusken, C. *Bull. World Health Organ* **2016**, *94* (8), 574−584D.

(21) Pinto, V. L., Jrunior; Luz, K.; Parreira, R.; Ferrinho, P. *Acta Med. Port.* **2015**, *28* (6), 760−765.

(22) Vorou, R. *Euro Surveill* **2016**, *21* (10), 30161.

(23) Liu, S. Q.; Li, X.; Deng, C. L.; Yuan, Z. M.; Zhang, B. *J. Med. Virol.* **2018**, *90* (3), 389−396.

(24) Musso, D.; Roche, C.; Nhan, T. X.; Robin, E.; Teissier, A.; Cao-Lormeau, V. M. *J. Clin. Virol.* **2015**, *68*, 53−5.

(25) Kaushik, A.; Tiwari, S.; Jayant, R. D.; Vashist, A.; Nikkhah-Moshaie, R.; El-Hage, N.; Nair, M. *Trends Biotechnol.* **2017**, *35* (4), 308−317.

(26) Qi, H.; Yue, S.; Bi, S.; Ding, C.; Song, W. *Biosens. Bioelectron.* **2018**, *110*, 207−217.

(27) Manzano, M.; Viezzi, S.; Mazerat, S.; Marks, R. S.; Vidic, J. *Biosens. Bioelectron.* **2018**, *100*, 89−95.

(28) Mills, D. M.; Calvo-Marzal, P.; Pinzon, J. M.; Armas, S.; Kolpashchikov, D. M.; Chumbimuni-Torres, K. Y. *Electroanalysis* **2017**, *29* (3), 873−879.

(29) Mills, D. M.; Martin, C. P.; Armas, S. M.; Calvo-Marzal, P.; Kolpashchikov, D. M.; Chumbimuni-Torres, K. Y. *Biosens. Bioelectron.* **2018**, *109*, 35−42.

(30) Mills, D. M.; Foguel, M. V.; Martin, C. P.; Trieu, T. T.; Kamar, O.; Calvo-Marzal, P.; Kolpashchikov, D. M.; Chumbimuni-Torres, K. Y. *Sens. Actuators, B* **2019**, *293*, 11−15.

(31) Kolpashchikov, D. M. *J. Am. Chem. Soc.* **2006**, *128* (32), 10625−8.

(32) Gerasimova, Y. V.; Hayson, A.; Ballantyne, J.; Kolpashchikov, D. M. *ChemBioChem* **2010**, *11* (12), 1762−8.

(33) Grimes, J.; Gerasimova, Y. V.; Kolpashchikov, D. M. *Angew. Chem., Int. Ed.* **2010**, *49* (47), 8950−3.

(34) Kolpashchikov, D. M. *Chem. Rev.* **2010**, *110* (8), 4709−23.

(35) Nguyen, C.; Grimes, J.; Gerasimova, Y. V.; Kolpashchikov, D. M. *Chem. - Eur. J.* **2011**, *17* (46), 13052−8.

(36) Gerasimova, Y. V.; Kolpashchikov, D. M. *Biosens. Bioelectron.* **2013**, *41*, 386−90.

DOI: 10.1021/acs.analchem.9b02455
Anal. Chem. 2019, 91, 13458−13464

(37) Labib, M.; Ghobadloo, S. M.; Khan, N.; Kolpashchikov, D. M.; Berezovski, M. V. *Anal. Chem.* **2013**, *85* (20), 9422−7.
(38) Labib, M.; Khan, N.; Berezovski, M. V. *Anal. Chem.* **2015**, *87* (2), 1395−403.
(39) Armbruster, D. A.; Pry, T. *Clin. Biochem. Rev.* **2008**, *29* (Suppl 1), S49−S52.
(40) Limit of Detection in Analysis. In *IUPAC Compendium of Chemical Terminology*, 2009.
(41) Gourinat, A. C.; O'Connor, O.; Calvez, E.; Goarant, C.; Dupont-Rouzeyrol, M. *Emerging Infect. Dis.* **2015**, *21* (1), 84−6.
(42) Mansuy, J. M.; Dutertre, M.; Mengelle, C.; Fourcade, C.; Marchou, B.; Delobel, P.; Izopet, J.; Martin-Blondel, G. *Lancet Infect. Dis.* **2016**, *16* (4), 405.
(43) Weusten, J. J. A. M.; Carpay, W. M.; Oosterlaken, T. A. M.; van Zuijlen, M. C. A.; van de Wiel, P. A. *Nucleic Acids Res.* **2002**, *30* (6), 26e.
(44) Reed, A. J.; Connelly, R. P.; Williams, A.; Tran, M.; Shim, B.-S.; Choe, H.; Gerasimova, Y. V. *Sens. Actuators, B* **2019**, *282*, 945−951.
(45) Abd el-Galil, K. H.; el-Sokkary, M. A.; Kheira, S. M.; Salazar, A. M.; Yates, M. V.; Chen, W.; Mulchandani, A. *Appl. Environ. Microbiol.* **2005**, *71* (11), 7113−6.
(46) Compton, J. *Nature* **1991**, *350* (6313), 91−2.
(47) Steinmetz, M.; Lima, D.; Viana, A. G.; Fujiwara, S. T.; Pessoa, C. A.; Etto, R. M.; Wohnrath, K. *Biosens. Bioelectron.* **2019**, *141*, 111351.
(48) da Fonseca Alves, R.; Franco, D. L.; Cordeiro, M. T.; de Oliveira, E. M.; Fireman Dutra, R. A. *Sens. Actuators, B* **2019**, *296*, 126681.
(49) Faria, H. A. M.; Zucolotto, V. *Biosens. Bioelectron.* **2019**, *131*, 149−155.

DOI: 10.1021/acs.analchem.9b02455
Anal. Chem. 2019, 91, 13458−13464